RE-VISITING YOLLA – MANAGING JACK-UP STORM STABILITY; GEOTECHNICAL ASSESSMENT

A. Amodio, C. Erbrich and V.Murugavel
Fugro AG Pty Ltd.

I. Moyle
Origin Energy Pty Ltd.

* *corresponding author: a.amodio@fugro.com*

1 ABSTRACT

In 2004 the Ensco 102 was spudded alongside the Yolla A platform in the Bass Strait, Australia. The uncemented silty carbonate soils at this site required a modified approach to documenting stability during storm events as discussed in Ref [1]. In early 2015 the Seadrill West Telesto was brought alongside the Yolla A platform with its spudcans re-penetrated deeply through the remoulded infill material within the existing craters. An extensive engineering exercise was commissioned to assess the storm stability for this new rig which involved a complex interaction between soil consolidation times and strength degradation under cyclic loads, coupled with uncertainty as to exactly what depth each of the spudcans would end up and hence what soil type they would rest on. A variety of anticipated scenarios were assessed, which included the effect of varying the installation preload, varying the return period of the storm and varying the VDL as a function of time. This paper will present the geotechnical work undertaken to unravel this complex puzzle, which led to a detailed installation flowchart that provided guidance on the process required to meet the acceptability criteria for each leg.

KEY WORDS: Yolla, Carbonate, Storm Stability, Consolidation, VDL Management, FLAC, Cyclic Strength

2 INTRODUCTION

The Yolla field is located in the Bass Strait, offshore Australia, due east of King Island and due North of Burnie, Tasmania. The field was first developed in 2004 with an unmanned platform (Yolla A), founded on a large skirted raft in order to produce gas for export by pipeline to Kilcunda in Victoria. The production wells for this platform were spudded in mid 2004 using the Ensco 102 jack-up rig, which was brought alongside Yolla A shortly after the platform installation. The three spudcans penetrated to between about 23 m and 24 m below mudline under the maximum applied preload, which was significantly deeper than expected. In addition, unexpected punch-throughs with long leg-runs were experienced leading to rig tilt and near collisions with the Yolla A platform. Following completion of drilling, the Ensco 102 was demobilised, resulting in the formation of large seabed craters.

Due to the substantial penetration depths achieved by the spudcans, the extraction operation was also complicated. In particular at the starboard leg substantial jetting of the soil was required to aid the leg extraction. As a result of these operations the crater soil was extremely remoulded and contained a variety of localised sandy pockets/ layers, which in most cases are presumed to have been formed by the washing out of fine material during the jetting process.

Recently, Origin Energy Resources Limited (Origin) has undertaken the Mid-life Enhancement (MLE) Project, which included an upgrade of the facilities onboard the Yolla A Platform and the drilling of additional wells. For the drilling operation, a JU 2000E class rig (Seadrill West Telesto) has been used for a new work-over operation in the existing craters. The West Telesto has a very similar spudcan layout and geometry as the Ensco 102 and was selected to minimise crater interaction issues.

The original Yolla operations were described in Ref [1], including an outline of the procedure adopted to estimate the spudcan capacity under storm loading conditions (i.e. the so-called 'Modified SNAME' approach). The same procedure was applied for the West Telesto assessment and the results from the various analyses conducted were used to prepare an installation flowchart. This was incorporated into the jack-up installation procedure and was used to help identify the acceptable criteria in terms of final penetration depth, applied preload, acceptable VDL and time required for consolidation. This flowchart and the analyses used to compile it are presented in this paper.

3 ACCEPTABILITY CRITERIA

The spudcan storm stability assessment performed for the West Telesto at Yolla was used to determine the maximum allowable Variable Deck Load (VDL) that the jack-up could support during various design storm events. The allowable VDL is defined by subtracting the factored dead weight and environmental loads from the jack-up foundation capacity. It increases with time as consolidation under the weight of the jack-up leads to strength gain in the soil; hence the most restrictive conditions (i.e. lowest allowable VDL) occurs just after the jack-up has been installed.

A minimum operable VDL was defined by the project team as about 1,100 tonnes, and under this condition two criteria were defined as representing acceptable outcomes:

i. At 'Time 0', the three spudcans were required to provide sufficient capacity against 1 yr return period seasonal (from Feb to March) storm conditions assuming the minimum operational VDL.
ii. Three days after jack-up installation, the spudcans were required to provide sufficient capacity against the 50 yr return period storm condition assuming the minimum operational VDL.

These criteria were defined considering that the weather requirement to commence the jack-up installation was a seven day outlook with a sea-state milder than the 1 yr seasonal storm condition. The estimated time required for installation of the three legs to final penetration was about 24 hours; hence the risk of a 50 yr storm condition occuring less than three days after final leg penetration was considered negligible.

If these conditions could not be met for any given final penetration depth then this would be deemed an unacceptable risk, and hence other mitigations might then be required. Prediction of the expected range of penetration depth was therefore a critical input to this work, and is presented in the companion paper Ref [2].

4 INSTALLATION FLOWCHART

Installation flowcharts were developed to aid decision making during the installation operation and to provide a simple definition of the procedure required to achieve acceptable criteria for each leg based on the final penetration depth achieved and the preload applied. The flowchart developed for the Starboard leg is presented on Figure 1; similar charts were also developed for the Port and Bow legs. In order to obtain an acceptable combination of final penetration depth and applied installation preload the maximum preload was generally limited to 90 MN, but under certain circumstances this could be increased to 100 MN. These limits were imposed to minimise the potential for a punch-through below a depth of 24 m as discussed in Ref [2].

It can be seen that the procedure prescribed an initial preload of 70 MN, which is the maximum preload that could be applied simultaneously to all the legs while keeping the hull in the water, with 5 m draft. The principal objective of this first stage was to reach the deepest penetration under all the three legs in the shortest time while mitigating any punch-through risk up to this preload level. Quick application of the preload also minimised the effect of rapid consolidation on the soil below the spudcans which at this stage (i.e. before an appropriate penetration depth had been reached), could locally increase the subsequent penetration resistance and increase the risk of punch-through thereafter.

During the second stage, the preload was increased independently on each leg with the ultimate objective to reach an acceptable penetration depth for inplace storm stability. Standard installation procedures typically require that the maximum preload should be held on each leg for about three hours after the final penetration is achieved, but in this case, for the first two legs, the preload was immediately downloaded as soon as the final penetration had been obtained in order to reduce the potentially detrimental effect of rapid consolidation on the penetration resistance of the remaining high legs.

For the Starboard Leg, the maximum preload adopted in this stage was 90 MN for which the minimum acceptable penetration depth was found to be 22 m. A similar procedure was adopted for the bow and port legs, but the analyses showed that the minimum acceptable depth at these legs was 23 m. A maximum allowable penetration depth of 30 m is also indicated on the flowchart which represents the highest credible penetration estimate in the event that the previous jack-up operations had led to undetected damage to the underlying formation.

If the minimum acceptable penetration depth were not achieved during the previous preloading stages then it was recommended to increase the preload in 1MN increments. This would be continued until the penetration had reached the minimum required penetration depth or until the preload had been increased to 100 MN. Provided that the penetration had reached at least 21 m by this point then the situation would be considered acceptable.

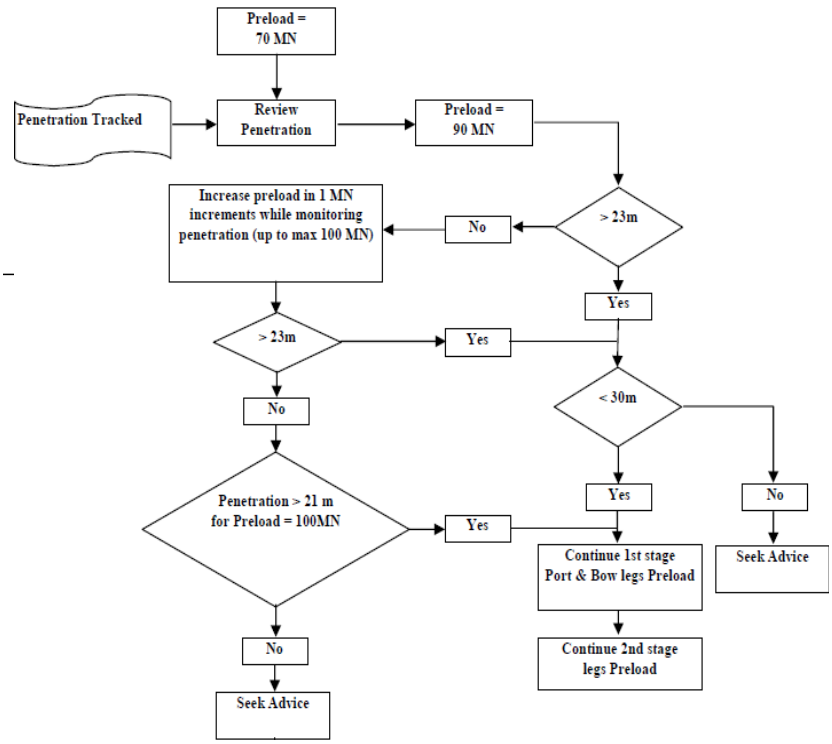

Figure 1 - Installation Flowchart for Starboard Leg

5 'VDL VERSUS CONSOLIDATION TIME' CHARTS

As already discussed, increasing consolidation time leads to a steady increase in the foundation capacity until full consolidation of the seabed is achieved; as a result the allowable VDL can increase with time if it is calculated based on the true spudcan capacity. However, in standard industry practice (i.e. SNAME; Ref [3] and ISO; Ref [4]) the spudcan capacity is determined based only on the preload applied during installation, with no consideration of the effect of consolidation strength gain (nor, on the opposite side of the equation, for strength degradation under cyclic loading). For the Yolla assessment, both the standard SNAME approach and the time dependent spudcan capacity have been applied, with the most conservative outcome selected at any particular time. The time dependent approach always governs at early times, but later when the effects of consolidation become dominant, the SNAME approach defined the VDL limits.

As input to the jack-up operational procedures, a set of curves were provided for each leg that define the allowable VDL for different consolidation time periods. Curves were derived considering a range of penetration depths and for a range of design storm conditions (i.e. 50 yrs, 1 yr 'all season' and 1 yr 'seasonal'). The curves for 50 yrs storm and 1 yr 'seasonal' conditions are presented on Figure 2a and 2b respectively. The VDL's presented in these charts define the allowable values for a specified longitudinal and transverse centre of gravity (e.g. for 50 yrs conditions, LCG = 0 m and TCG = -1.4 m respectively), while for any other position of the centre of gravity the allowable VDL was derived from VDL contours charts which were developed using the results on Figure 2, by DNV-GL (see companion paper, Ref [5]). Figure 3 presents a typical VDL contour chart

for the 50 yrs storm conditions, where the value for each contour was defined assuming the allowable VDL at the specified centre of gravity (i.e. LCG = 0 m and TCG = -1.4 m) to be equal to the Maximum Allowable VDL of 2,500 tonnes. Once the jack-up installation had been concluded the leg which resulted in the lowest allowable VDL would be used in the VDL management process for the subsequent drilling operations.

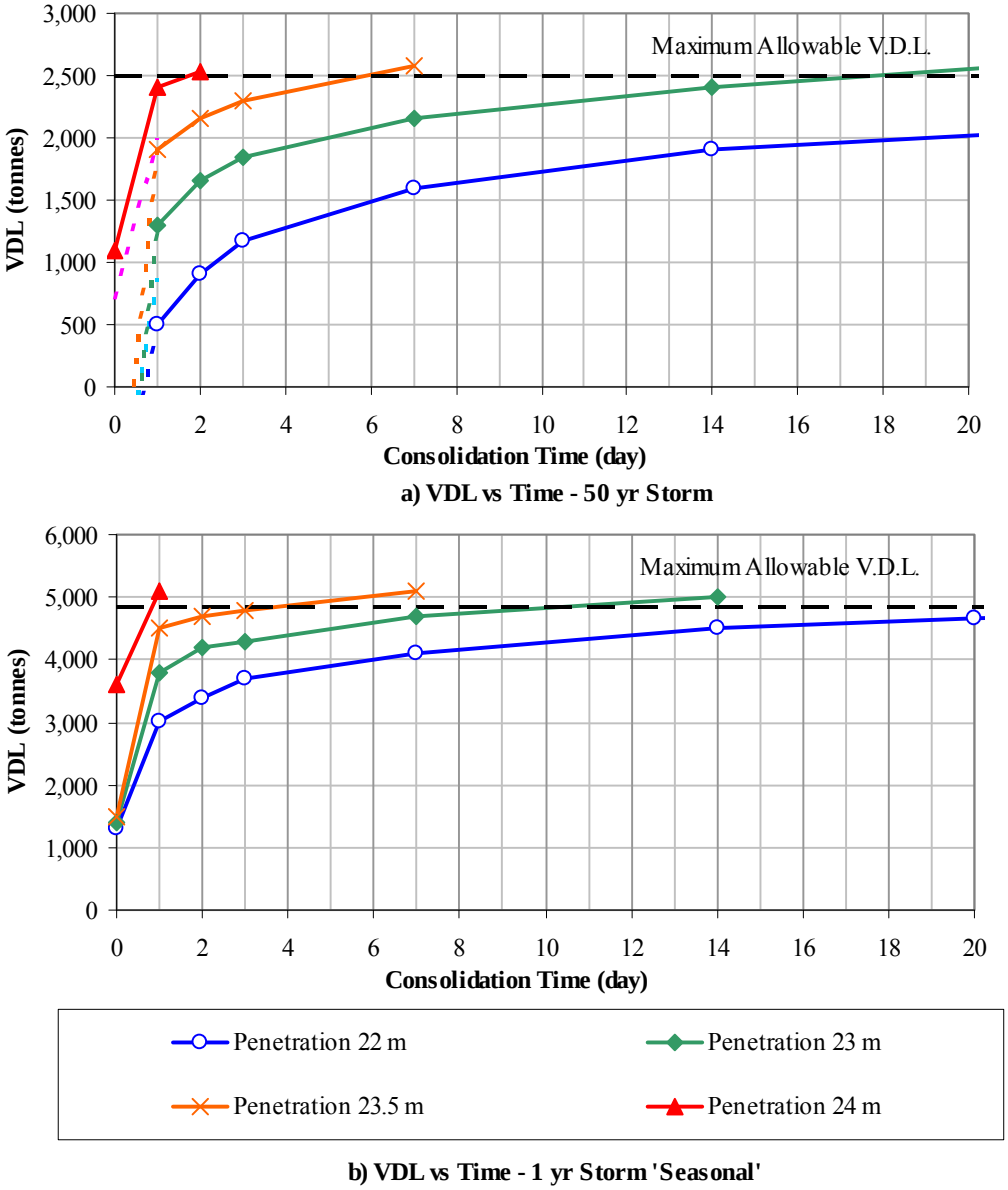

Figure 2 - VDL vs Consolidation Time Charts

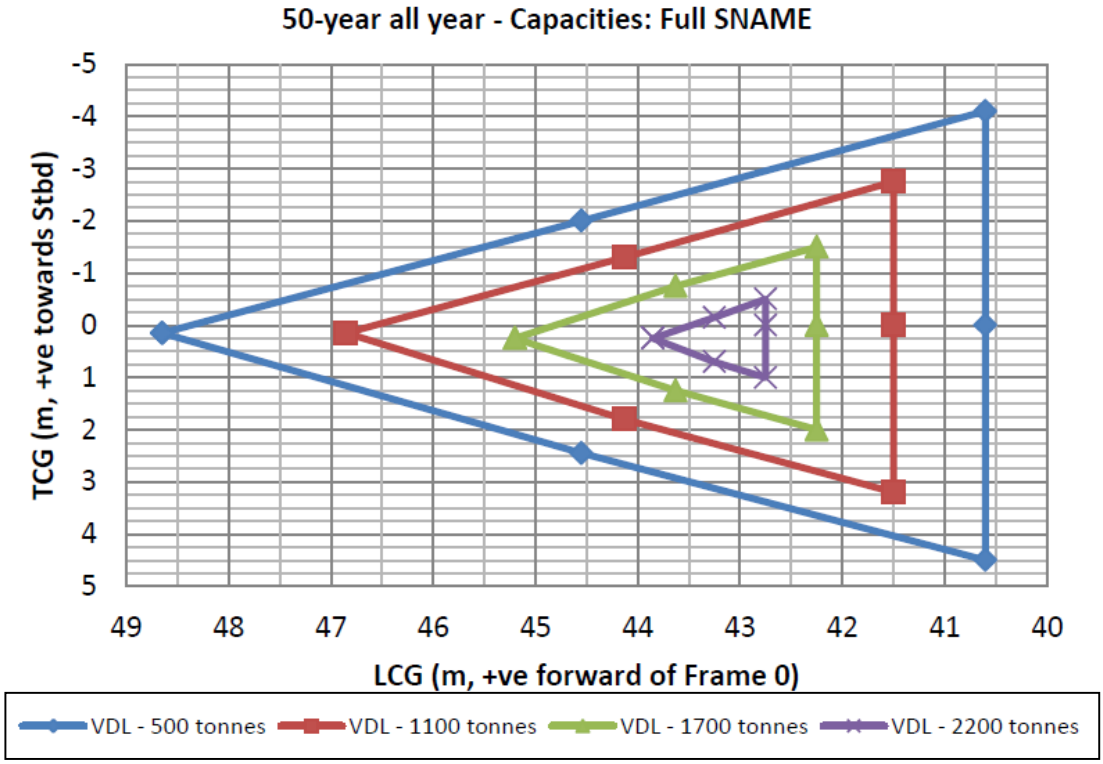

Figure 3 - VDL Contours with Allowable LCG -TCG Envelopes for 50 yrs Storm

6 SOIL CONDITIONS - GENERAL

The soil conditions at each leg are presented in detail in Ref [2]. The in situ material is laterally homogeneous but exhibits significant variability with depth. The site generally comprises a variety of interbedded layers of uncemented carbonate sand/ silty sand/ sandy silt but also includes a number of calcareous clay layers. A typical in situ CPT profile, annotated with the stratigraphy, is shown on Figure 4. The penetrometer results in the carbonate silty sand/ sandy silt layers exhibit varying degrees of partial drainage which complicates interpretation of the strength.

The first investigation of the crater infill material comprised a single CPT probe through the centre of each crater, along with static and cyclic ball penetrometer tests in the port and bow craters. The CPT response obtained in each of these craters is presented on Figure 5. It can be observed that there is significant variability between the three craters, with the starboard crater exhibiting a typically sandier response than the other two craters. The greater presence of sand in this crater was thought to be due to the more extensive use of jetting during extraction of the Ensco 102 spudcan compared to the other craters. Initial analyses indicated a punch-through risk at this crater during re-penetration and hence it was decided to collect additional data from this location, which comprised a series of CPT's scattered across the crater (Figure 6). Figure 7 illustrates the results from these additional investigations. It can be seen that while the original centre CPT exhibits the greatest prevalence of sand, significant zones of potentially interconnected sand exist across the crater.

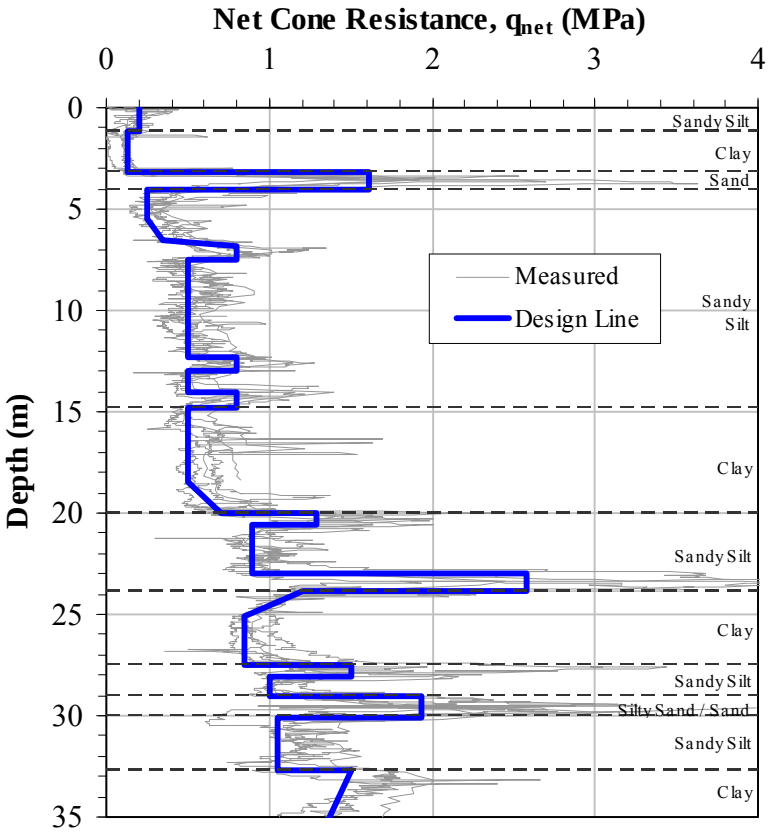

Figure 4: A Typical In-situ CPT Profile

From these results it can be concluded that the soil in the existing three craters was significantly remoulded and remixed up to about 23 m below mudline during the original operations, which is approximately the final penetration depth achieved by the Ensco 102. The in-situ strength profile shows a layer of silty sand between 23 m and 24 m and this appears partially disturbed below the craters, presumably during the leg extraction. However, below this layer the original soil conditions appear largely intact.

Ref [2] describes the approaches used to assess the appropriate strength of the various soil layers during spudcan penetration. Allowances were made for the varying degree of partial drainage in different layers that would apply during spudcan penetration. However, under storm conditions the load is applied much faster than during leg installation and under these conditions fully undrained conditions apply in all layers. Calculation of the undrained strength is presented later in this paper.

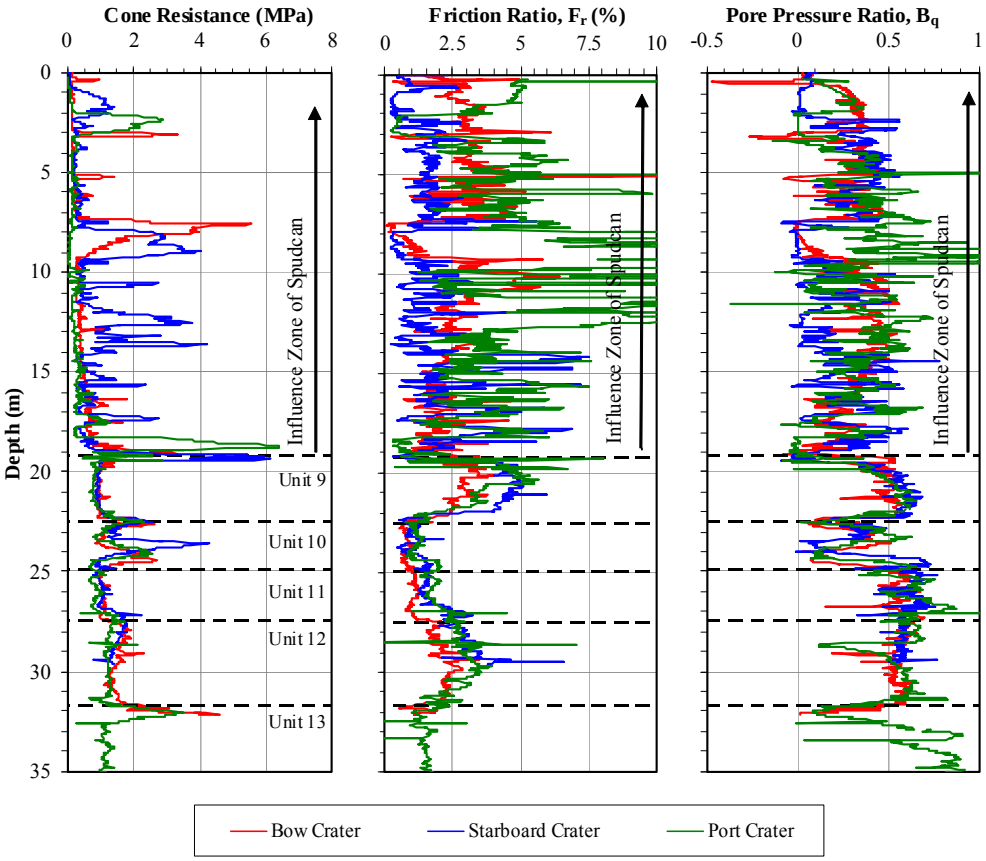

Figure 5: CPT response obtained in Bow, Starboard & Port Crater

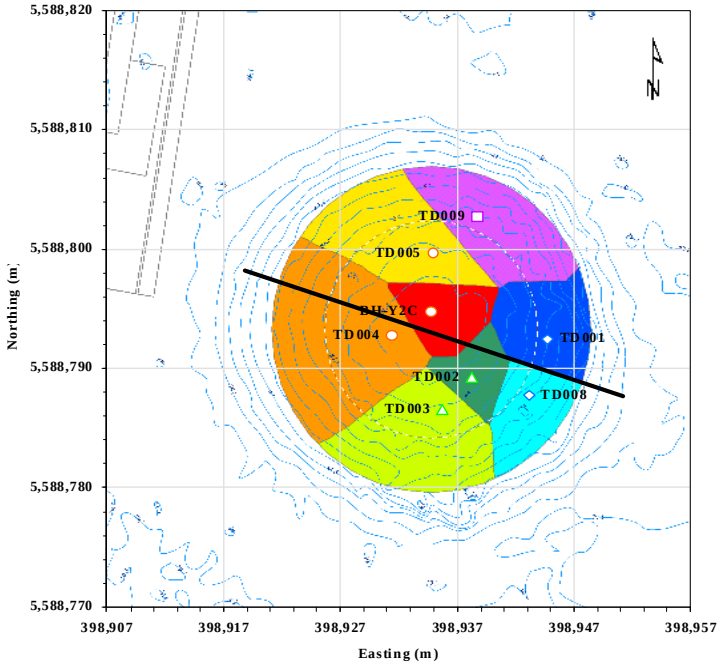

Figure 6: Starboard Crater: CPT location

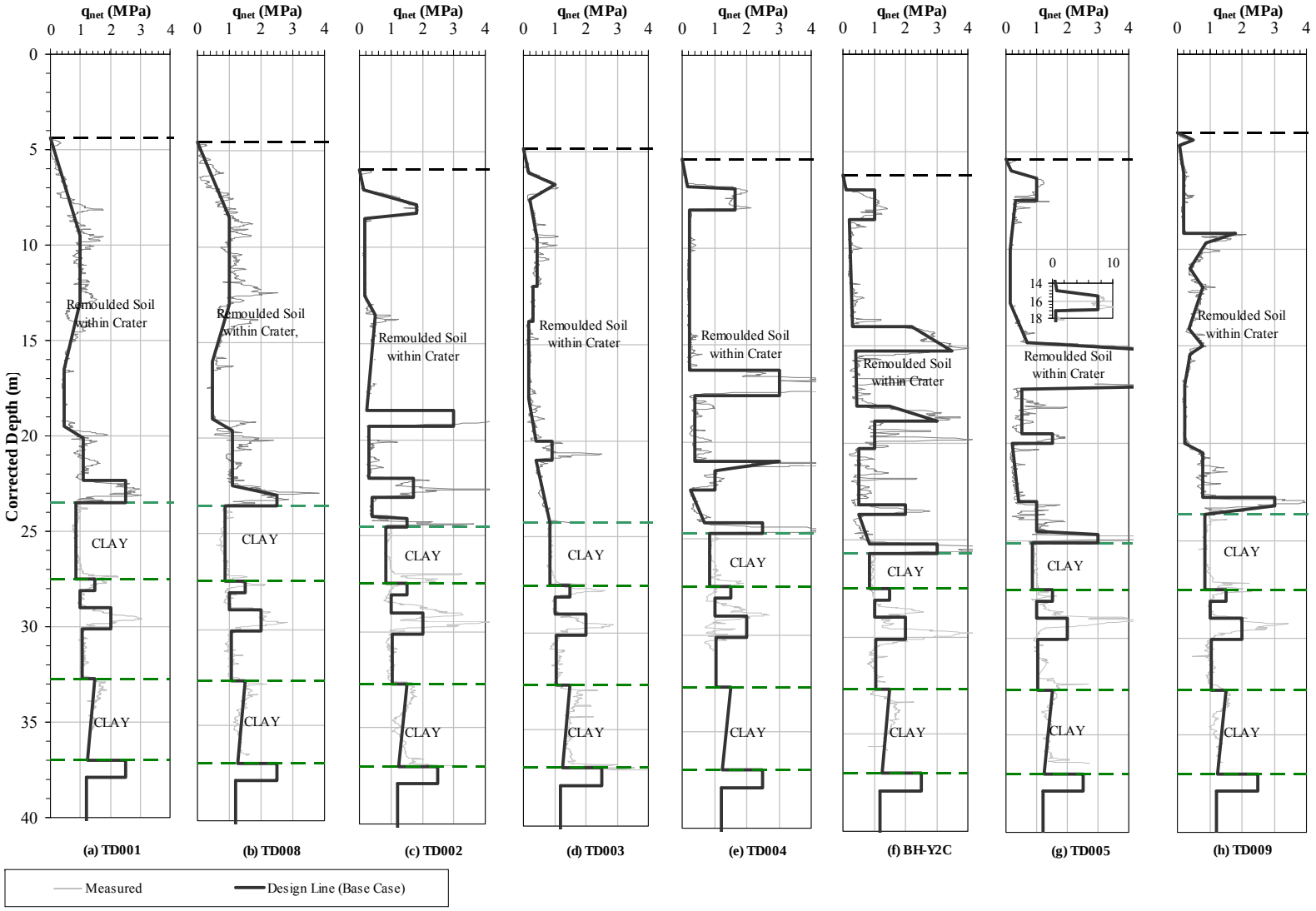

Figure 7: Additional PCPT Data Obtained Within Starboard Crater (refer to Figure 6 for CPT locations)

7 STORM STABILITY ANALYSIS

The acceptability criteria, installation flowcharts and VDL management criteria have already been described and presented. The remainder of this paper will therefore describe the analyses that were used to define the storm stability limits that form the basis of the results presented earlier.

8 METHOD OF ANALYSIS - GENERAL

In order to assess the spudcan storm capacity for any analysed condition (i.e. particular combination of penetration depth, maximum applied preload, and storm condition) the following steps have been followed:

i. Calibration of the soil strength profile during penetration
ii. Assessment of undrained monotonic shear strength profile
iii. Assessment of undrained cyclic consolidated soil strength profile
iv. Calculate vertical and horizontal spudcan cyclic capacity
v. Apply modified SNAME approach to assess the allowable VDL
vi. Define the VDL vs. consolidation time charts
vii. Verify the acceptability criteria

Each of these steps is summarised below.

Calibration of the Soil Strength Profile during Penetration

The starting point for each spudcan capacity analysis at any given penetration depth is that the spudcan must, by defintion, be in a state of static equilibrium under the maximum imposed preload. In order to ensure this is achieved in our analysis, the soil strength profile adopted during the installation (which account for some degree of partially drained behaviour), was adjusted in some specific layers (by factoring up or down) through a calibration exercise such that the monotonic spudcan bearing capacity at the selected depth was very close to the target preload. The calibrated strength profile resulting from this exercise was therefore defined as $s_{u,s,cal} = s_{u,s} \cdot \eta$, where η is the calibration factor and $s_{u,s}$ is the design strength originally assigned. The calibration factor was applied only to layers which were considered to be the principal cause of uncertanty in the definition of the strength profile, such as the remoulded soil above 23 m.

Undrained Monotonic Shear Strength

The soil strength defined from the above calibration process incorporates partial drainage effects and hence must be modified in order to account for the fully undrained behaviour which is expected during storm loading. The installation strength profile was maintained unchanged for all layers where fully undrained behaviour was assumed during the preload operation. However for all layers which were considered to behave partially drained during the leg penetration a correction factor was applied to the installation strength to obtain the fully undrained strength. The layers subject to this correction were the sandier layer between 23 m and 24 m and the sandier pockets within the starboard crater.

Consolidated Monotonic and Cyclic Shear Strength

Consolidation analyses were perfomed in order to assess the degree of consolidation within the soil at various times after installation. The analyses were performed using an axi-symmetric model in the geotechnical finite difference program, FLAC (Ref [6]). The coefficient of consolidation, c_v adopted in these analyses is presented on Figure 8.

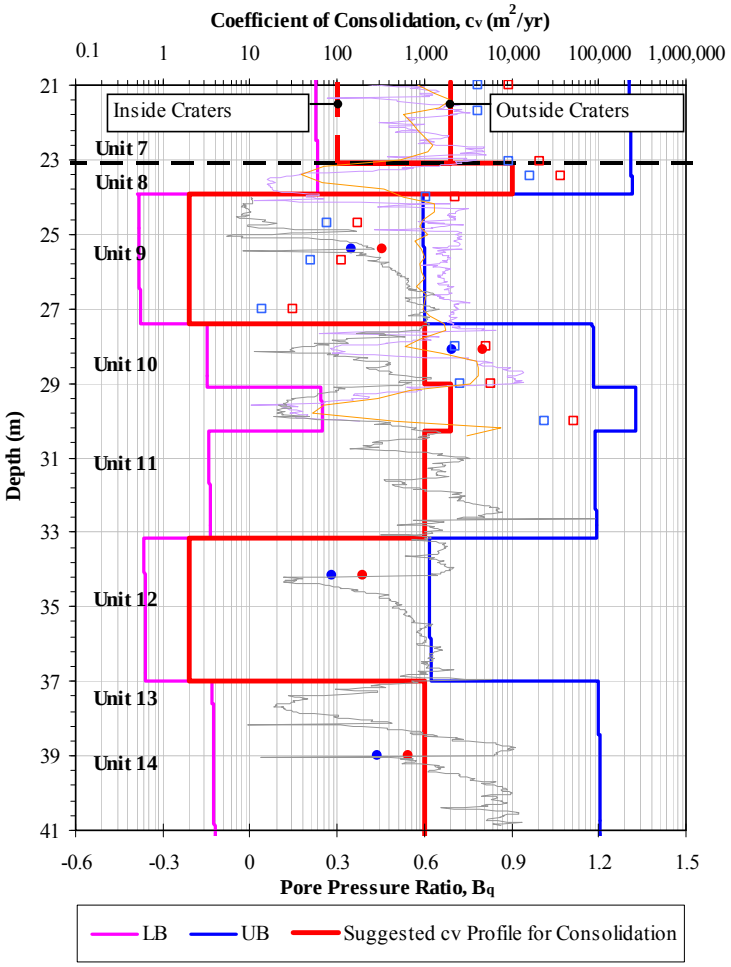

Figure 8: Coefficient of Consolidation adopted in the Consolidation Analyses

The relationship used to compute the consolidated monotonic shear strength has been described in Ref [7]:

$$\frac{s_{u-mono}}{\sigma'_{vi}} = J\sigma'^{\,n}_{vi} \geq L \qquad (1)$$

where n and J are empirical coefficients, L is the normally consolidated cut-off and $s_{u\text{-}mono}$ and σ'_{vi} are in kPa. The *n* parameter used with this model in the current case was calibrated from site specific consolidated simple shear tests (i.e. $n = -0.06 \cdot \ln(s_u/\sigma'_{vi})_{25kPa} - 0.61$). For each element in the model, the increment in vertical effective stress ($\Delta\sigma'_v$) considered in the calculation of the consolidated strength gain was assumed to be equal to the increment in vertical total stress ($\Delta\sigma_v$) times the degree of consolidation (U):

$$\Delta\sigma'_v = \Delta\sigma_v \cdot U. \qquad (2)$$

The strength degradation induced by the cyclic nature of the storm loads was also considered in the final spudcan capacity calculation following the approach described in

Ref [7] but calibrated to the results of cyclic simple shear tests performed on the different soil units found at Yolla. The results are presented in terms of the ratio of the cyclic strength to monotonic strength ($s_{u\text{-}cyc}/s_{u\text{-}mono}$) as a function of ($s_{u\text{-}mono}/\sigma'_{vi}$):

$$\frac{s_{u-cyc}}{s_{u-mono}} = a \exp\left(b \frac{s_{u-mono}}{\sigma'_{vo}} \right) + c \qquad \leq 1.0 \tag{3}$$

where a, b and c are empirical parameters which apply to a given number of cycles, N, and $s_{u\text{-}cyc}$ is defined as the strength mobilized at 15% shear strain.
The form of this equation (Figure 9) invariably indicates increasing degradation for higher normalised monotonic strengths (i.e. for higher $s_{u\text{-}mono}/\sigma'_{vo}$).

The cyclic strength is defined as the mobilised strength at a peak cyclic shear strain of 15 % at an appropriate number of load cycles and for a given cyclic load ratio (CLR). The CLR is defined as τ_{cyc} / τ_{ave}, where τ_{cyc} is the shear stress generated by the cyclic component of the applied load and τ_{ave} is the shear stress generated by the monotonic component of the applied load along the failure surface. The CLR can be calculated on an element-by-element basis (i.e. for each element of the adopted model) or as the average value along the failure surface using the method described in Ref [8]. For the work described in this paper the average CLR value was adopted in the calculation. In lieu of a full storm history analysis for this case it was assumed that the design storm events could be conservatively represented by 30 cycles of the peak storm load.

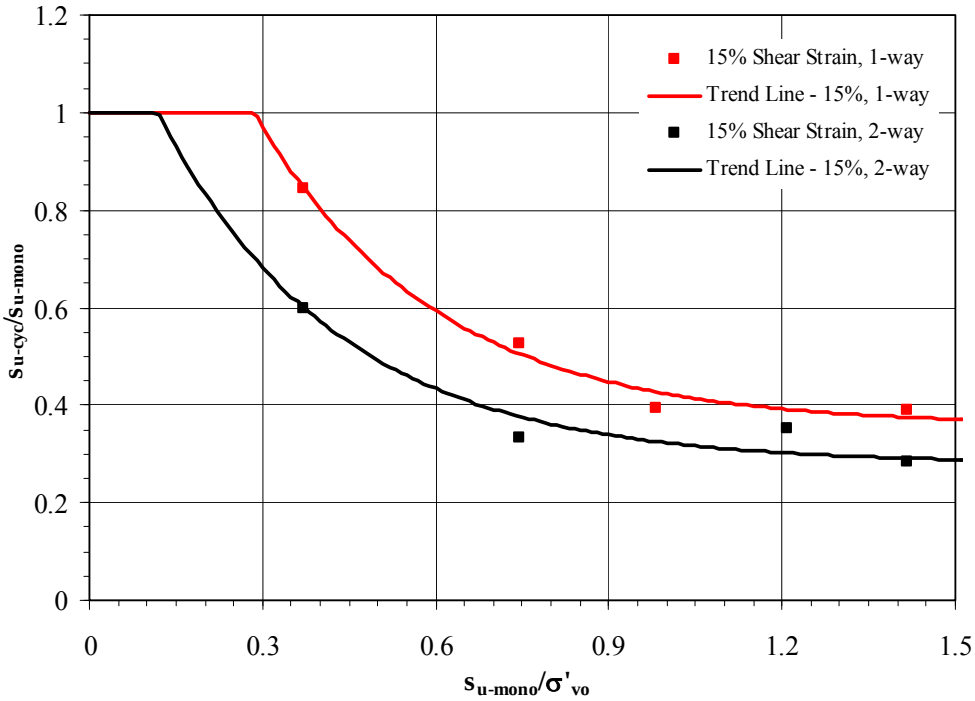

Figure 9: Cyclic Undrained Shear Strength, N_{eq}=30

The combined effect of consolidation strength gain and cyclic degradation is presented on Figure 10 for a specific spudcan configuration (i.e. final penetration of 23 m and applied preload of 90 MN).

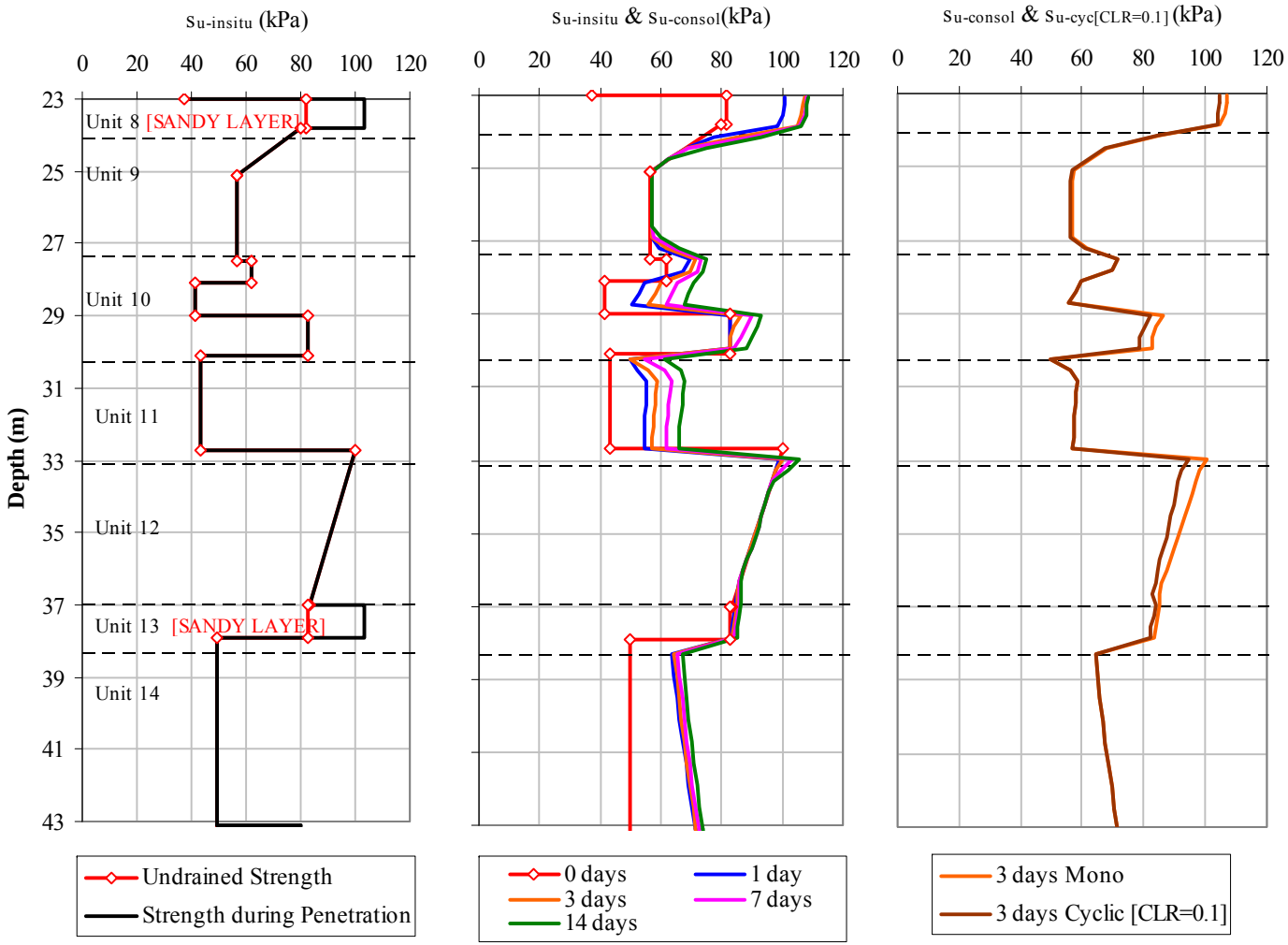

Figure 10: Soil Strength, Combined Effect of Consolidation Strength Gain and Cyclic Degradation

Modified Sname Approach and Allowable VDL Calculation

The 'Modified SNAME' approach proposed in Ref [1] has been used to assess the foundation capacity for each case considered. In the classical SNAME approach the preload is used to define the pure vertical capacity. This is then used in turn to anchor the combined load yield envelope from which the applicable material factor under storm loads is determined. In the 'Modified SNAME' approach the measured preload is replaced with the calculated vertical capacity, accounting for consolidation and cyclic degradation. Since a calculated rather than measured capacity is now used to anchor the combined load yield envelope, a higher required material factor is also specified; 1.25 in this case which is consistent with 'conventional' design practice for most offshore shallow foundations. In these analyses the VDL is varied until a minimum material factor of 1.25 is obtained for all three jack-up legs. The minimum VDL required to meet the minimum material factor requirement then defines the minimum allowable VDL for each specific case under consideration.

Pure Vertical and Horizontal Capacity

The pure vertical bearing capacity of the spudcans required for the 'Modified SNAME' approach was calculated using an axi-symmetric model in FLAC. These analyses were performed at various consolidation times and using the appropriate cyclic strength for the design event under consideration.

The pure horizontal capacity, which is also used to anchor the combined load yield envelope was calculated according to the method recommended in Ref [4] which includes three components: i) the sliding resistance component at the bottom of the spudcan; ii) the sliding resistance component at the top of the spudcan, in the remoulded soil and iii) a passive resistance component. The pure horizontal capacity (Q_H) is therefore calculated as:

$$Q_H = (s_{u,a} + s_{u,b}) \cdot A + K_P \cdot s_{u,s} \cdot A_s \qquad (4)$$

where:

$s_{u,a}$	=	Operative undrained shear strength of material above the spudcan;
$s_{u,b}$	=	Operative undrained shear strength at deepest depth of maximum bearing area;
$s_{u,s}$	=	Average operative undrained shear strength between the deepest depth of maximum bearing area and the top of the spudcan;
A	=	Spudcan effective bearing area based on cross-section taken at uppermost part of bearing area in contact with soil;
A_s	=	Spudcan laterally projected embedded area;
K_P	=	Coefficient of passive resistance, assumed equal to 7.02, according to the deep penetration case recommended in Ref [4].

9 STARBOARD LEG SPECIFIC ANALYSES - GENERAL

The spudcan penetration assessment (Ref [2]) revealed that the most likely final penetration depth for all three legs was about 24 m which is approximately the final penetration reached during the installation of the Ensco 102. The potential for shallower penetration at the bow and port leg was also considered, allowing for the possibility that the strength of the remoulded soil above 24 m might prove to be stronger than initially anticipated.

Specifically, final penetration depths between 22 m and 25 m were assessed in developing the final installation flowchart.

At the starboard leg the various PCPT's performed within the existing crater identified pockets of sandier material at various depths which were not observed at the other two legs. These pockets appeared to be largely discontinuous, but it was believed that there was a risk that as the West Telesto spudcan penetrated through these pockets they might gradually 'clump' together to form a monolithic unit of sandier material leading to premature refusal of the spudcan or to an unexpected punch-through event. As discused in Ref [2], large deformation finite element (LDFE) analyses were performed to assess these risks using the ABAQUS CEL capability. Three scenarios were considered in the LDFE starboard leg penetration assessment:

i. 'Scenario 1': All the soil units were treated as undrained/ partially drained with all strengths defined using a 'cohesive' material model;
ii. 'Scenario 2': The sandy units were modelled as a frictional material while the rest of the soil was modelled undrained/ partially drained with strengths defined using a 'cohesive' material model;
iii. 'Scenario 3': Same as 'Scenario 1' but with a reduced rate of remoulding for the undrained soil.

The results of the LDFE spudcan penetration analyses are summarised on Figure 11. It can be seen that two of the three scenarios (i.e. 'Scenario 2' and 'Scenario 3') resulted in significantly shallower penetration than obtained from the base case analytical model (results also shown).
It may be noted that for Scenario 1 the final predicted penetration at a preload of 90 MN is approximately 23 m. This is similar to the previous Ensco 102 penetration, and is similar to the predictions for the other two legs. The cyclic capacity assessment for this case can therefore be assumed the same as at the other two legs at the same spudcan penetration and hence no special treatment is required. However, the final predicted penetration for Scenario 2 and Scenario 3 reduces to 21 m and 18.5 m respectively, which are outside of the range predicted for the other two legs, and hence these cases must be considered seperately.

In practice it would not be possible to ascertain whether the cause of any observed shallow penetration less than 23 m was the specific soil conditions pertaining to Scenario 2 or something between Scenario 2 and 3. Hence under a 50 year storm, in order to confirm that a penetration depth of 21 m (for example) were acceptable under a 90 MN preload, we would first need to confirm that an acceptable VDL could be achieved using the soil conditions applicable to the LDFE analysis for Scenario 2. This is a necessary (but not sufficient) step, and hence the first set of analyses performed (Case 1), specifically considered this case. However, an acceptable VDL was not obtained for this case and hence these specific design conditions (i.e. 21 m penetration and 90 MN preload) could not be considered acceptable.

To address this problem, we therefore also considered the impact of increasing the preload up to 100 MN in the event of inadequate penetration under 90 MN preload, which was predicted to increase the penetration to 21 m for Scenario 3. We only considered Scenario 3 (i.e. the shallowest case) for this analysis since a positive outcome implies a similar or better outcome if the soil response is closer to Scenario 2 (noting that for this latter scenario, application of 100 MN preload increases the penetration to > 23 m). Hence

a positive outcome represents a necessary and sufficient condition to confirm acceptability in this case. To summarise, the following two set of analyses were performed for the starboard leg assessment:

i. Case 1: Strength profile from Scenario 2 (LDFE) – 90 MN preload – 21 m penetration depth
ii. Case 2: Strength profile from Scenario 3 (LDFE) – 100 MN preload – 21 m penetration depth

For both cases the spudcan storm capacity has been assessed considering the effect of strength gain under the static self weight of the rig as a function of consolidation time.

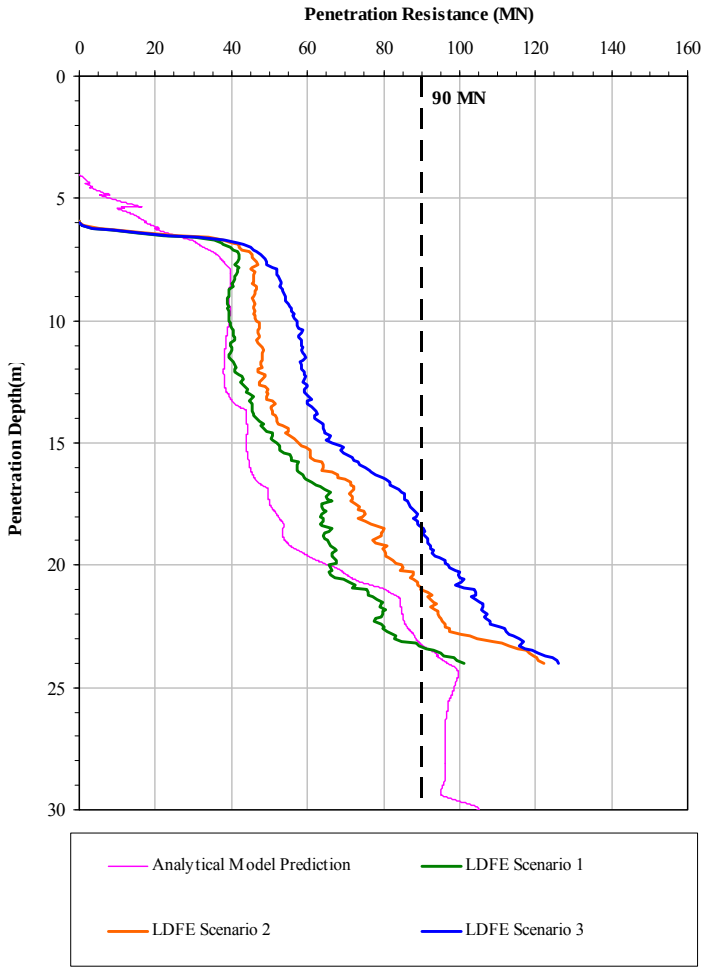

Figure 11: Results of the LDFE Spudcan Penetration Analyses

10 STARBOARD LEG SPECIFIC ANALYSES - METHOD

The ABAQUS LDFE penetration analyses were performed using a fully 3D model of the soil and spudcan. However, the general storm stability procedure outlined earlier is based on 2D (axi-symmetric) models to define the pure vertical capacity. It was therefore necessary to develop a procedure that could incorporate the complex 3D soil strength data

from the LDFE analyses into a form that would be compatible with the 2D storm analysis procedure.
The storm stability analysis for the starboard crater therefore comprised the following steps:

i. Extract a detailed 3D soil strength map from the ABAQUS CEL starboard model.
ii. Define equivalent axi-symmetric soil models which could each represent one soil strength sector (i.e. a region of soil that could be treated as having a single strength profile).
iii. Select representative sectors from the 3D soil strength map and define the consolidated cyclic undrained strength profile to adopt for each representative sector.
iv. Calculate vertical and horizontal spudcan cyclic capacity for each representative sector
v. Apply Modified SNAME approach and assess the allowable VDL
vi. Define VDL vs. consolidation time charts
vii. Verify the acceptability criteria

The processes required for each step are described below.

Step i) Extraction of 3D Soil Strength Map.
Using the 3D LDFE results for the spudcan at 21 m (i.e. the reference depth considered for all cases in this study), a large number of vertical probes were first performed through the model, with the operative soil strength profile extracted from each, within the area of interest around the spudcan. The 3D LDFE model was divided into 12 circumferential sectors (6 from the northern half model and 6 from the southern half) each comprising 4 annuli (two within the spudcan footprint; probe 1 and 2 and two in the laterally adjacent remoulded zone; probe 3 and 4) to create 48 equal area zones at each plan level as shown on Figure 12. The vertical probes were performed at the centre of each zone and the extracted strength was then assumed to apply over the entire plan area of that zone.

For the Case 2 analysis the strength probes were performed using the results from the Scenario 3 LDFE analysis where all the soil was modelled with a cohesive post peak strain-softening model. The information extracted from this case comprised the operative undrained shear strength for each material type within any element intersected by the probe and the percentile of each material type within that element. The latter is required since the soil is allowed to move (flow) from one element to another in the 3D LDFE analyses. Initially, each mesh element is assigned a single soil 'type' (e.g. 'intact', 'silty sand', 'clay', etc.). However, as the analysis proceeds the soil can flow from one element to another so over time each element may contain material of more than one type, each of which contributes to the average strength that applies.

For Case 1, the probes were performed using the results from the Scenario 2 LDFE analyses. For this scenario, all materials were modelled as cohesive post peak strain-softening, except for the sandier layers, which were modelled using frictional properties. For the storm capacity analyses undrained strengths are required for all material types, and hence the appropriate undrained shear strength (s_u) assigned to these sandier zones was extracted instead of the frictional properties. The information extracted from each probe for this case therefore comprised the percentile of each material in any element intersected by the probe and the undrained shear strength for each material type. However, for the

sandier material the peak strength was adopted for this case rather than the operative strength, since 'remoulding' doesn't occur for material that behaves in a drained frictional manner during penetration.

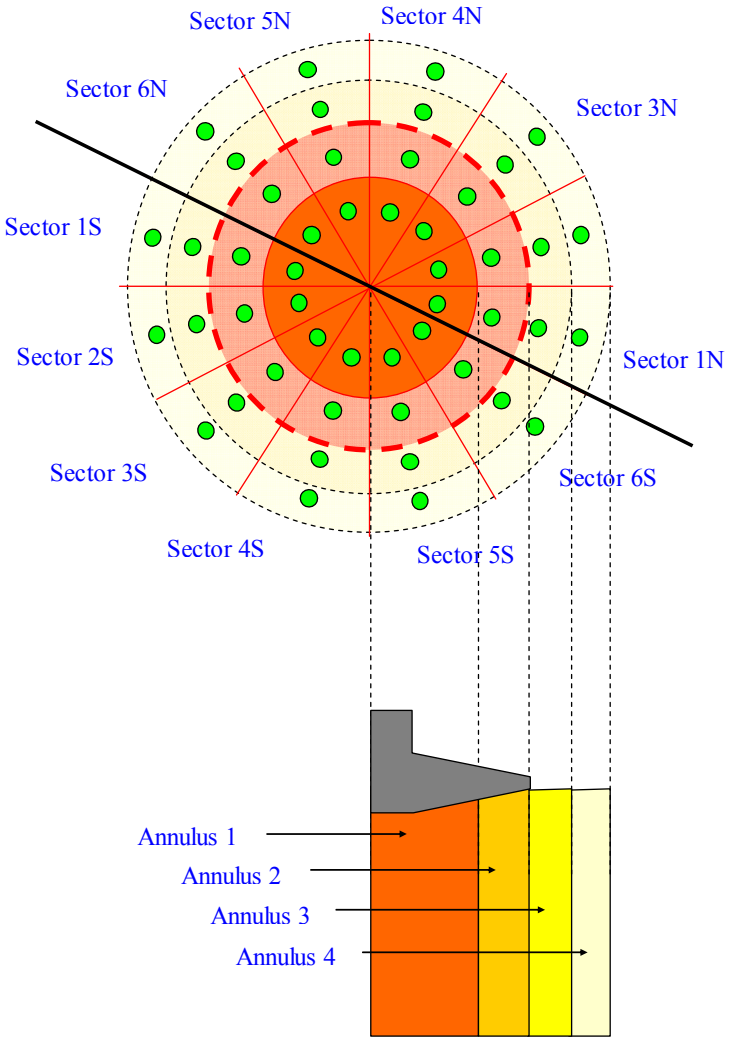

Figure 12: Subdivision of 3D LDFE Model into Annuli and Sectors

For both Case 1 and 2, for every element along each probe, a weighted 'average strength' was calculated based on the percentage of each material type and its corresponding shear strength.

Typical strength probe results obtained are presented on Figure 13 for Case 1; in this case we have selected four sectors at 90° intervals to illustrate the variability in operative strength obtained.

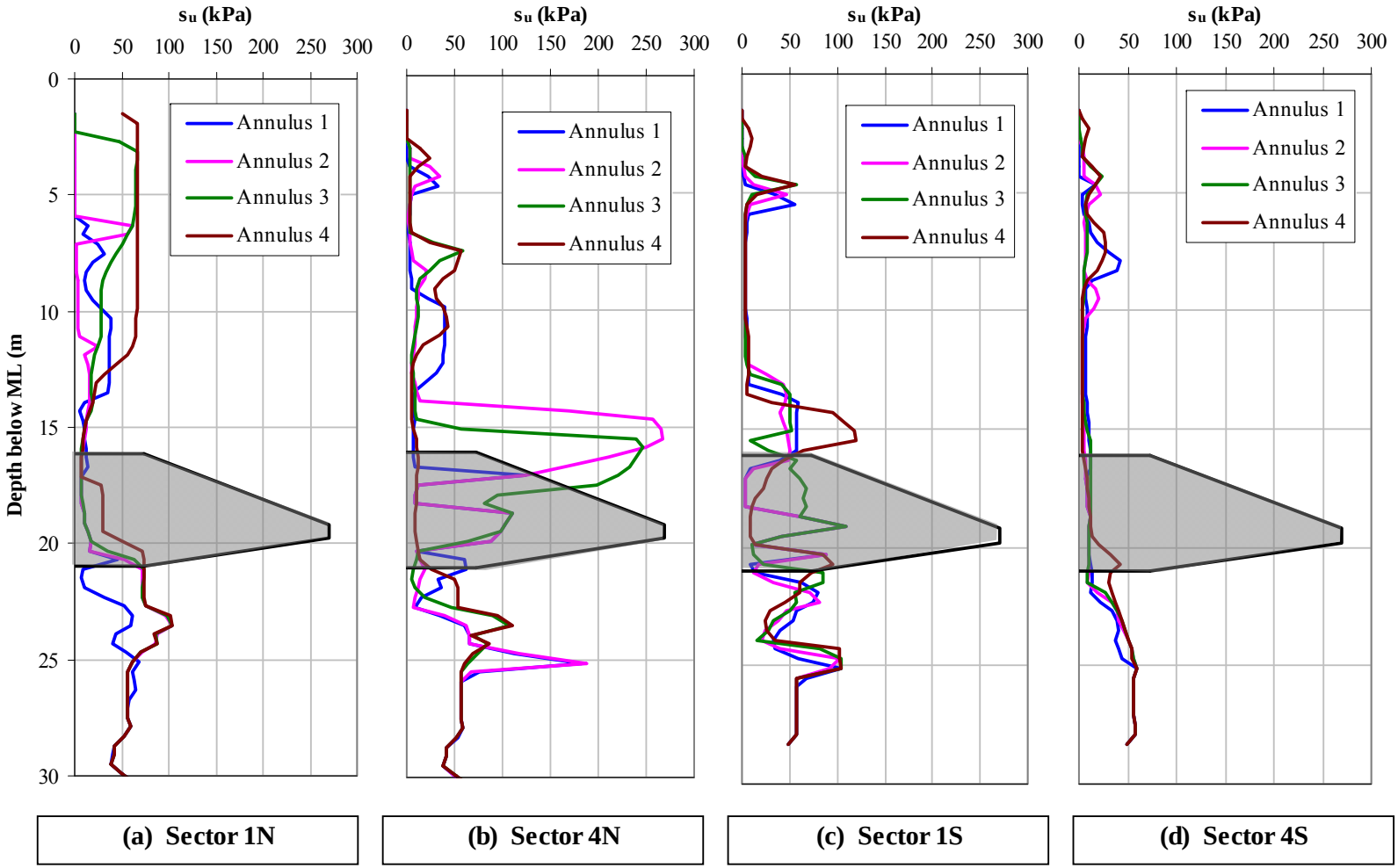

Figure 13: Strength Profile for Selected Envelopes

Step ii) Definition of Axi-symmetric Soil Models

Since the FLAC capacity analyses are based on an axi-symmetric model of the soil and spudcan, it is not possible to simultaneously model the 3D soil strength distribution resulting from the 48 separate zones at each plan level. Initially we therefore generated a single simplified profile that we thought could apply in a single axi-symmetric model, by using the average strength determined from the individual strengths that were extracted around the circumference for each element in the FLAC grid. However, this resulted in a monotonic capacity that was much higher than the preload applied in the LDFE model (which was by definition at incipient failure) and hence it was concluded that such a simple approach was not suitable. To address this problem we therefore generated 12 individual axi-symmetric models, each representing the specific soil profile applicable to one circumferential sector. The monotonic vertical capacity was then calculated for each sector individually.

Step iii) Selection of Representative Sectors and Strength Definition

Owing to the substantial variability in soil strength between each sector, the results of the individual monotonic analyses revealed large differences in the ultimate vertical capacity. Consistent with the initial simplified case, it was found that the average of these individual capacities was well above the preload applied in the original 3D LDFE model. This finding implied that the ultimate failure mechanism in the full 3D model focused on a preferential failure surface that developed within the weakest material zones. Since only a single sector can be considered in an axi-symmetric model, the sectors which gave capacities closest to the 3D reference capacities (Q_{ref}) were chosen as the representative sectors. These would be expected to define the closest approximation to the governing 3D failure mechanism.

After a representative sector had been selected for each case, the corresponding soil strength profiles were scaled such that the capacity of the FLAC axi-symmetric model exactly equaled Q_{ref}.

For Case 2, the Scenario 3 LDFE analysis is the reference case, where the soil strength is modelled as cohesive (undrained or partially drained) in all units. This is the same assumption as made in the FLAC axi-symmetric calculation and hence the monotonic capacity of the FLAC model must equal the capacity from the 3D model; in this case Q_{ref} therefore equals the applied preload of 100 MN at 21 m.

For Case 1, the calibration process was not so straightforward since the Scenario 2 LDFE analysis is the reference case. For this scenario, the sandier units were modelled as fully drained with frictional properties adopted in the LDFE analysis, whereas the FLAC model is based on cohesive undrained/ partially drained strengths in all layers, which implies a lower capacity. The appropriate reference capacity from the 3D models to use in this case would be somewhere between the applied preload of 90 MN in Scenario 2 and the reaction observed at the same depth in Scenario 1 (i.e. 75 MN; see Figure 11), where the strength of the sandier layers was modelled assuming cohesive material with a high rate of post-peak strain softening. Conservatively, we selected the lower bound of this range (i.e. 75 MN) as Q_{ref} for calibrating the FLAC axi-symmetric model.

The individual sector results obtained from the FLAC axi-symmetric model are presented on Figure 14 for Case 1 and 2, with the selected representative sector shown for each case.

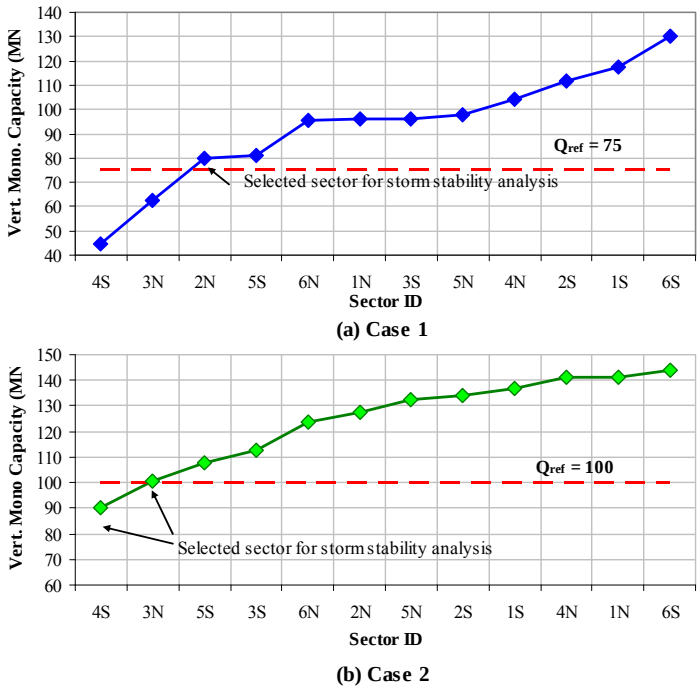

Figure 14 Individual Sector Results Obtained From The FLAC Axi-Symmetric Model

Step iv) to Step vii)

All the remaining steps in the storm analysis procedure (i.e. from step iv to step vii) were the same as for the standard analyses performed for the bow and port craters, as described earlier. The only difference was that the representative sectors with appropriately scaled strength were used as the input profiles for the storm stability analyses.

11 TYPICAL STORM STABILITY RESULTS

A large number of different storm stability analyses were performed in order to define the results required to parameterise the installation flowcharts for each crater and the VDL management tool. Herein we present results from one case as a typical example; Starboard crater Case 1. Figure 15 presents the degree of consolidation obtained at various times up to 14 days after installation. Figure 16 presents a contour plot showing the consolidated cyclic undrained shear strength, assuming a CLR of 0.1 for the selected representative sector (2N) at the same time intervals. This figure also includes displacement vectors revealing the ultimate pure vertical failure mechanism. CLR values varying between 0.09 and 0.18 were calculated for different legs and storm conditions, with the strength degradation calculated each time accordingly; however a value of approximately 0.1 was calculated for the most critical leg. Note that for simplicity, the spudcans were modeled as flat plates in these analyses with the embedment depth chosen to equal the penetration depth of the widest section of the actual spudcan. After calculating the pure horizontal capacity, and processing the loads through the SNAME yield function, the VDL that met the required material factor was determined for each case. These results were in turn then converted into the requirements presented in the installation flowchart and VDL vs consolidation time charts, as illustrated on Figure 1 and 2 respectively.

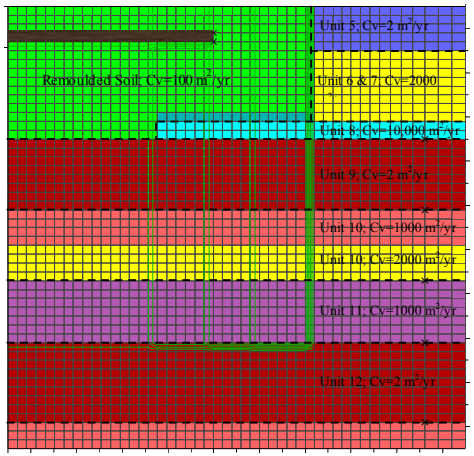

(a) Coefficient of Consolidation

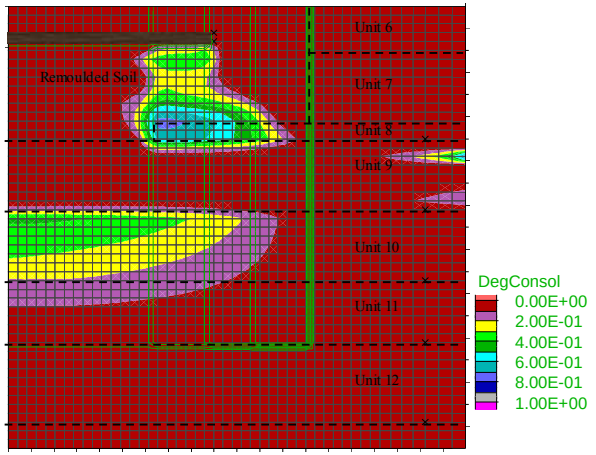

(b) Time - 3 day

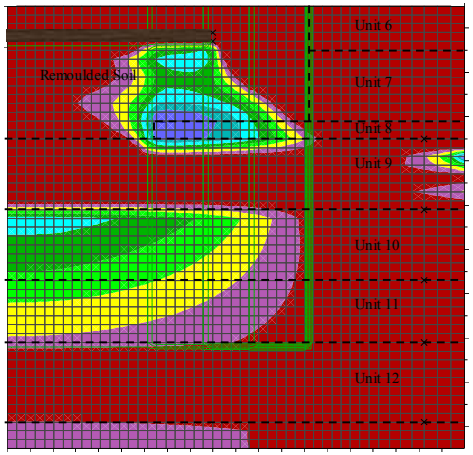

(c) Time - 7 day

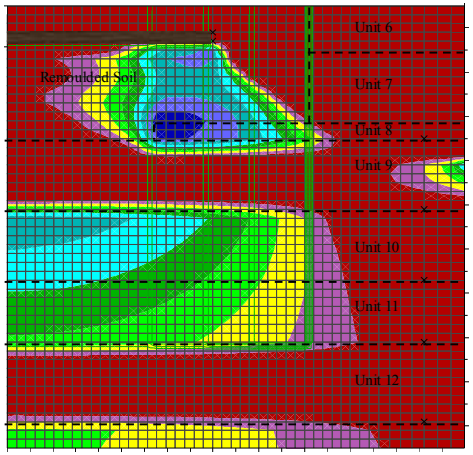

(d) Time - 14 day

Figure 15 Starboard Crater Case 1: Degree of Consolidation Contours

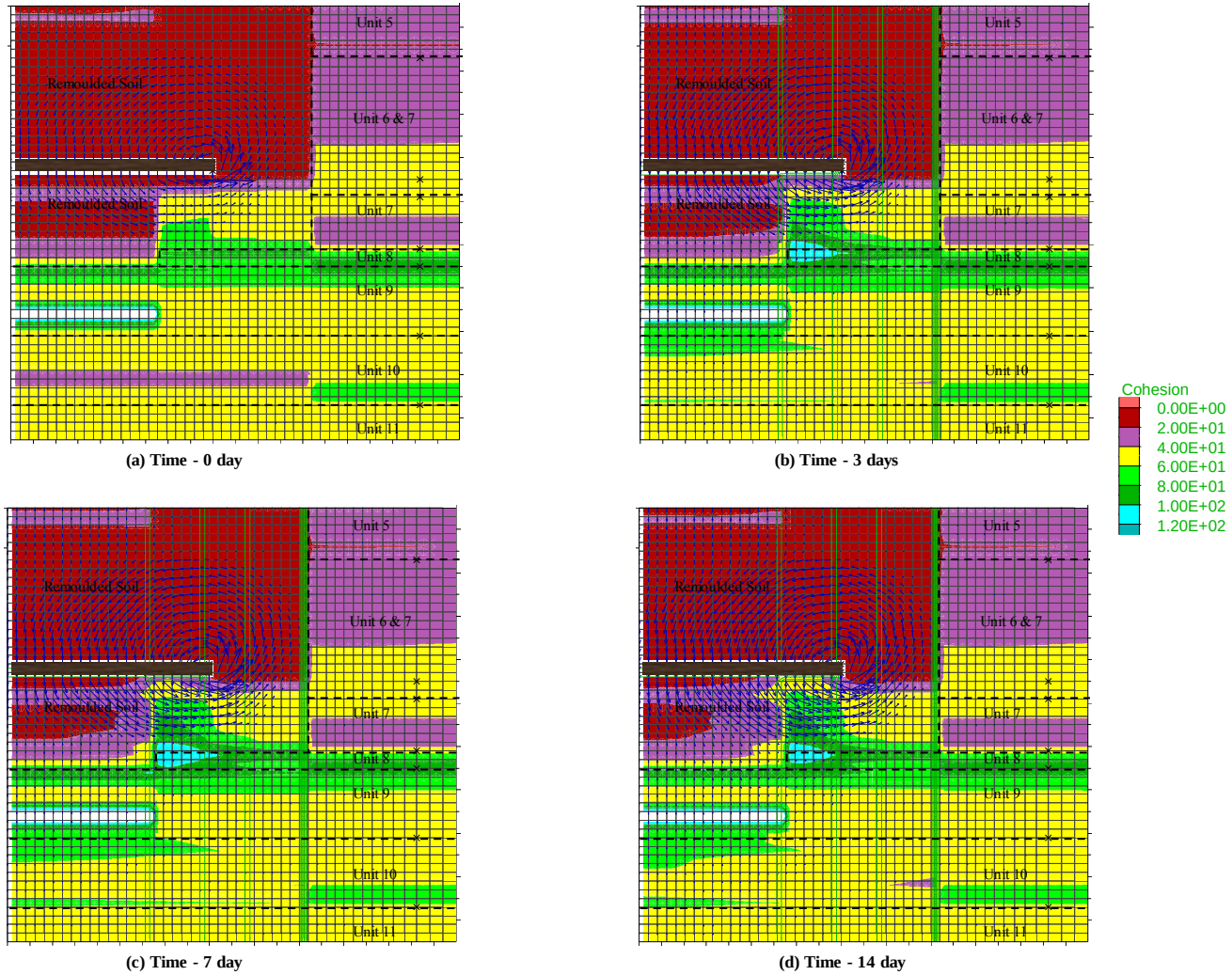

(a) Time - 0 day **(b) Time - 3 days**

(c) Time - 7 day **(d) Time - 14 day**

Figure 16 Starboard Crater Case 1: Strength Contours and Failure Mechanism

12 OBSERVED WEATHER CONDITIONS AND VDL MANAGEMENT

The West Telesto Jack-up was successfully installed at Yolla on the 28 February 2015. The final penetration for the Bow, Port and Starboard leg were respectively 22.8 m, 22.0 m and 24.2 m and the VDL was managed during the subsequent drilling operations in accordance with the results presented on Figure 2 for a penetration depth of 22.0 m.

Five days after installation a significant weather event occurred at the site, with the bad weather lasting for two days (i.e. the 5th and the 6th of March 2015). During this period the maximum significant wave height (H_s) was measured as 5.7 m, which is close to the seasonal 1 yr return period storm (H_s=6.3 m). During this period the VDL was managed according to the VDL management curve provided for the 1 yr 'seasonal' conditions.

Another significant weather event was recorded between the 6th and 13th of May 2015 when two large storms occurred at the site with a one week interval. The maximum H_s for the first storm had a recorded maximum H_s = 7.0 m (i.e. which is equivalent to a 10 yr return period storm for the month of May or a 1 yr return period 'all year' storm), while the maximum recorded H_s for the second storm was 6.4 m, which is close to the seasonal 1 yr return period storm. Figure 17 shows the observed H_s between the 04 May and 14 May; Figure 18 shows a photo taken from the rig during the storm of 05 May. The wave height was recorded at a buoy approximately 28 km to the west of Yolla A which is more sheltered from westerly weather than the platform; hence the sea state at Yolla A may have been slightly worst than recorded at the buoy. For this event the VDL was managed according to the VDL management curves provided for the 1 yr return period 'all year' storm (H_s=7.0 m) with some additional conservatism added to account for the possibility of cumulative damage due to the close proximity of these two storms.

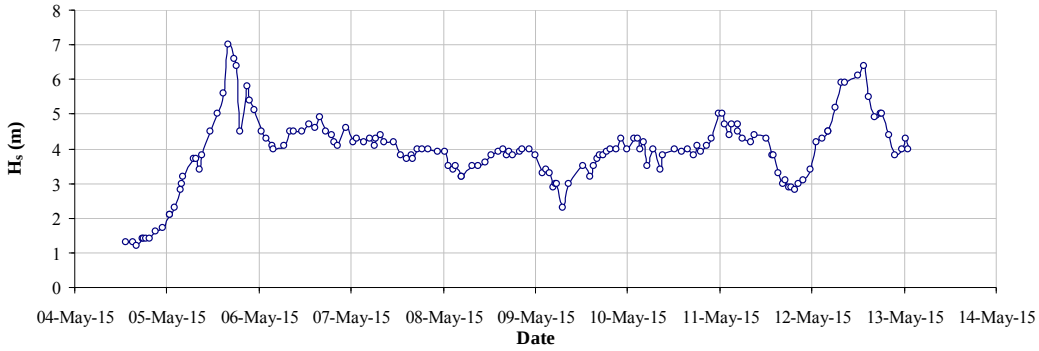

Figure 17 Observed H_s between the 04 May and 14 May

13 CONCLUSIONS

The work presented in this paper was conducted as part of a comprehensive engineering evaluation that may be unprecedented in the history of global jack-up installations. The lessons learnt from the surprises and near-miss that occurred with the E102 in 2004 were well learnt and no stone was left unturned to minimise the risk of undesirable outcomes this time.

The complexity of the soil conditions, comprising highly sensitive carbonate silty soils with transitional drainage conditions, required an intense engineering exercise to assess the

storm stability for each potential installation scenario. These results were used to provide guidance on the process required to meet the acceptability criteria for each leg and were used as input to a VDL management tool which defined limits to the permissible VDL during severe environmental events. It was not long before these tools were tested in action, with several severe weather events encountered during the drilling operations including both 10 year and 1 year return period 'seasonal' storms in May 2015. The West Telesto survived all these events with no evidence of any adverse effects, which is due testament to the engineering effort that was undertaken for this drilling campaign.

Figure 18 Photo from Heli-Deck during the Storm of 5 May 2015 (Courtesy of Origin Energy)

14 ACKNOWLEDGEMENTS

The authors would like to thank the BassGas Joint Venture partners for permission to publish this paper. Origin Energy is the Operator of the BassGas Joint Venture in permit T/L1.

The BassGas Joint Venture partners in T/L1 are:

Origin Energy Resources Limited (Operator)	42.50%
AWE Limited (via subsidiaries)	35.00%
Toyota Tsusho Gas E&P Trefoil Limited	11.25%
Prize Petroleum International Pte. Ltd	11.25%

The success of the West Telesto operations at Yolla can be attributed to the team Origin put together for this exercise, and the contributions made by DNV-GL, Halliard Consulting, Seadrill and the various technical experts from the Yolla partners are acknowledged.

15 REFERENCES

[1] Erbrich CT. Australian Frontiers – Spudcans on the Edge. in: Proceedings, The International Symposium on Frontiers in Offshore Geotechnics (ISFOG). Australia, 2005. p 49-75.

[2] Erbrich CT, Amodio A, Lam, S, Krisdani H., Lam S. and Xu X. and Tho K.K., Re-visiting Yolla – New Insights on Spudcan Penetration. in: Proceedings, International Conference: The Jack-up Platform. London, UK, 2015.

[3] SNAME. Guidelines for Site Specific Assessments of Mobile Jack-up Units. The Society of Naval Architects and Marine Engineers. New Jersey, 2008.

[4] International Standards Organisation (2011). Petroleum and Natural Gas Industries – Site-Specific assessment of mobile offshore units – Part 1: Jack-ups.

[5] Moyle I, Hayward M., Rahman Z., Zhang Y., Tools for Managing VDL Limitations in Challenging Australian Soil and Environmental Conditions in: Proceedings, International Conference: The Jack-up Platform. London, UK, 2015.

[6] Itasca (2011). 'FLAC: Fast Lagrangian Analysis of Continua', User Manual, Itasca Consulting Group.

[7] Amodio A., Chang T.M., Kong V. & Erbrich CT, The Effects of Jack-up Installation Procedures on Spudcan Capacity in Offshore Carbonate Sediments (ISFOG 2015) p 1253-1260.

[8] Randolph, M.F. and Erbrich, C.T. (2000), Design of Shallow Foundations for Calcareous Sediments, Proceedings of the 2nd International Conference on Engineering for Calcareous Sediments, Bahrain, Feb 1999, Ed. Shafei KA, Balkema.